Structure of Trimethyldioxorhenium, $(CH_3)_3ReO_2$, As Studied by Spectroscopic Methods, Gas Electron Diffraction, and Density Functional Theory Calculations. Tilted Methyl Groups: Agostic C−H···M Interactions or Bent M−C Bonds?

Arne Haaland,* Wolfgang Scherer,*,† Hans Vidar Volden, and Hans Peter Verne

Department of Chemistry, University of Oslo, Box 1033 Blindern, N-0315 Oslo, Norway

Odd Gropen

Institute of Mathematical and Physical Sciences, University of Tromsø, N-9037 Tromsø, Norway

G. Sean McGrady

Department of Chemistry, King's College London, Strand, London WC2R 2LS, U.K.

Anthony J. Downs and Gereon Dierker

Inorganic Chemistry Laboratory, University of Oxford, South Parks Road, Oxford OX1 3QR, U.K.

Wolfgang A. Herrmann, Peter W. Roesky, and Martin R. Geisberger

Anorganisch-chemisches Institut der Technischen Universität München, Lichtenbergstrasse 4, D-85747 Garching bei München, Germany

Received June 1, 1999

The structural model of the trimethyldioxorhenium molecule, Me_3ReO_2 (**1**), has been revised on the basis of analysis of its ^1H, ^{13}C, and ^{17}O NMR and vibrational spectra and of its gas electron diffraction (GED) pattern. The results are consistent with the molecular symmetry C_s; in the new model both oxo ligands together with one methyl group are located in the equatorial plane of a distorted trigonal bipyramid. Structure optimization by density functional theory (DFT) calculations and least-squares refinement to the GED data yield the valence angles (calc/expt; eq = equatorial; ax = axial; av = average) $\angle C_{eq}ReO = 118.0/118.5(10)°$ and $\angle C_{eq}ReC_{ax} = 74.3/73.5(11)°$. The pseudoaxial Re−C bond distance is found to be shorter than the equatorial one, viz., $Re-C_{ax} = 2.130/2.122(6)$ Å versus $Re-C_{eq} = 2.193/2.199(22)$ Å, and $Re{=}O_{av} = 1.739/1.703(3)$ Å. It is suggested that the distortion from trigonal bipyramidal to edge-bridged tetrahedral coordination geometry is driven by the need for the axial C atoms to achieve optimal overlap with both the d_{z^2} and d_{yz} orbitals on the Re atom. The DFT calculations indicate that the axial methyl groups are tilted in such a manner that the ∠ReCH valence angles in the ReC_3 plane are reduced to 100.8°. It is suggested that this tilting is due in part to bent $Re-C_{ax}$ bonds and in part to weak C−H···Re agostic interactions.

1. Introduction

Since the discovery of an efficient synthesis of methyltrioxorhenium, $MeReO_3$, in 1988, it has been shown that this molecule is a very useful catalyst for several reactions, including the oxidation of olefins and aromatic systems, the Baeyer Villiger oxidation, metathesis reactions, and the olefination of aldehydes.[1] These widespread applications in catalysis have motivated us to carry out detailed investigations on the only other known methylrhenium(VII) oxide, namely, trimethyldioxorhenium(VII), **1**. An oil at room temperature, **1** was first synthesized by Mertis and Wilkinson[2] by oxidation of tetramethyloxorhenium(VI) with nitrogen monoxide. It may also be obtained by oxidation of hexamethyltrioxodirhenium(VI) with trimethylamine-*N*-oxide (eq 1).[3]

$$[Me_3(O)Re]_2O + Me_3NO \rightarrow 2Me_3ReO_2 + Me_3N \quad (1)$$

Only a handful of other triorgano-dioxorhenium compounds are known, viz., R_3ReO_2, where $R = CH_2CMe_3$,[4a]

† Present address: Anorganisch-Chemisch Institut der Technischen Universität München.

(1) Romão, C. C.; Kühn, F. E.; Herrmann, W. A. *Chem. Rev.* **1997**, *97*, 3197−3246.

(2) Mertis, K.; Wilkinson, G. *J. Chem. Soc., Dalton Trans.* **1976**, 1488−1492.

(3) Herrmann, W. A.; Romão, C. C.; Kiprof, P.; Behm, J.; Cook, M. R.; Taillefer, M. *J. Organomet. Chem.* **1991**, *413*, 11−25.

(4) (a) Cai, S.; Hoffmann, D. M.; Wierda, D. A. *J. Chem. Soc., Chem. Commun.* **1988**, 313−315. (b) Cai, S.; Hoffmann, D. M.; Wierda, D. A. *Organometallics* **1996**, *15*, 1023−1032.

10.1021/om9904201 CCC: $19.00
Publication on Web 12/10/1999

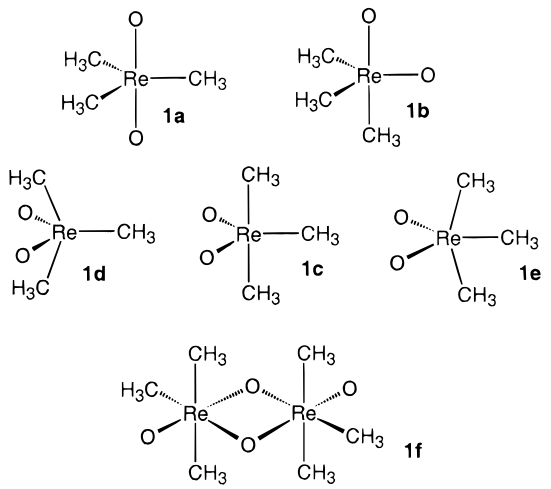

Figure 1. Possible molecular structures for Me_3ReO_2, **1**.

2, or CH_2SiMe_3[4a] and $R(Me_3CCH_2)_2ReO_2$, where R = Me,[4b] CH_2SiMe_3,[4b] or Ph,[4b] **3**.

Unless the oxo ligands in Me_3ReO_2 are disposed *trans* to each other—a most unlikely situation given the strongly π-bonding nature of these groups[5]—then either the oxo ligands or the methyl groups *must* occupy inequivalent coordination sites in a trigonal bipyramidal (TBP) or square pyramidal (SQP) framework. On the evidence of the IR and ^{1}H NMR spectra of **1**, Mertis and Wilkinson ruled out a TBP structure with both O atoms in axial positions, **1a** (see Figure 1), and proposed instead a TBP structure with one oxygen atom located in an axial and the other in an equatorial position, **1b**.[2] Here we show by reference to the ^{1}H, ^{13}C, and ^{17}O NMR spectra of solutions, to the vibrational spectra, and to the gas electron diffraction (GED) pattern of the vapor that **1** is a monomeric compound with a severely distorted trigonal bipyramidal framework in which *both* oxygen atoms take up pseudoequatorial positions, **1e**.

Similar structures were deduced by single-crystal X-ray diffraction studies of the neopentyl derivative **2**[4a] and the mixed neopentyl/phenyl derivative **3**.[4b] It has been suggested on the evidence of the X-ray model and of the NMR spectroscopic properties that the former may be stabilized through α-C_{ax}−H···O=Re interactions. Neither DFT calculations nor the NMR and vibrational spectra give any grounds for invoking similar interactions in the methyl derivative **1**.

2. Results and Discussion

2.1. NMR Spectrosopic Studies of Me_3ReO_2 in Solution. Chloroform-d_1 solutions of **1** show two sharp signals in the ^{1}H and ^{13}C NMR spectra with intensities in the ratio 2:1; the relevant chemical shifts are $\delta(^1H)$ = 2.47 and 2.03 ppm; $\delta(^{13}C)$ = 26.7 and 29.7 ppm, respectively. These signals, unlike the corresponding features of **2**,[4a] do not change significantly with temperature. The ^{17}O NMR spectrum of **1** in the same solvent displays only one signal [$\delta(^{17}O)$ = 756 ppm] and is thus incompatible with a distorted TBP structure with one equatorial and one axial O atom, **1b**, as proposed by Mertis and Wilkinson.[2] The NMR spectra are equally consistent with a TBP structure with both O atoms in equatorial positions, **1c**, with a SQP with the O atoms at opposite corners of the base, **1d**, or with **1e**, which Ward and co-workers[6] have referred to as an edge-bridged tetrahedron (EBT). The C_3O_2 coordination polyhedra of these models all have C_{2v} symmetry. **1c** is converted into **1d** through distortion along a Berry pseudorotation coordinate and into **1e** through distortion along the inverse of the pseudorotation coordinate.

A hypothetical dimeric structure for **1** with the two bridging oxygen atoms, **1f**, may also be ruled out since the bridging oxygen would be expected to lead to an additional signal in the ^{17}O NMR spectrum in the range δ = 200−400 ppm.[7a,b] Aggregation can also be discounted on the evidence of the CI-MS spectrum, which reveals a molecular peak corresponding only to the monomeric form, with no sign of a fragment including two or more rhenium atoms. In the following account we will present a structural model for **1** based on an analysis of GED results and DFT calculations. NMR−GIAO calculations based on the optimum DFT model of **1** give chemical shifts in reasonable agreement with the experimental values (Table 1). Comparison with the monoalkylated oxorhenium species $MeReO_3$, **4**, and $EtReO_3$, **5**, reveals calculated and observed ^{17}O chemical shifts for **1** that clearly occur at lower frequency in contrast with the behavior of the ^{13}C NMR signals associated with both types of C_α atoms in **1**.

2.2. IR and Raman Spectrosopic Studies of Me_3ReO_2. These studies sought evidence (i) of agostic α-C−H···Re interactions or (ii) of α-C−H···O=Re interactions of the type indicated by the crystal structure of **2**.[4a] A full vibrational assignment for several isotopomers of **1**, including force field calculations and normal-coordinate analysis, will be the subject of a subsequent publication;[8] here we concentrate on the vibrational spectrum of the naturally occurring $(CH_3)_3ReO_2$ species and its deuterated counterpart $(CD_3)_3ReO_2$ in light of the stated aims and report the IR spectra of the matrix-isolated molecules and the Raman spectra of liquid samples. Major features are detailed in Table 2. In the following discussion, details of the spectra of $(CD_3)_3ReO_2$ are given in parentheses.

(i) Methyl Group Internal Modes. A manifold of C−H (C−D) stretching vibrations occurs at 3025−2860 (2275−2105) cm^{-1}. Methyl deformations appear in two groups: δ_{as} at 1470−1385 (1080−1020) and δ_s at 1255−1190 (945−905) cm^{-1}. Features in the region 825−750 (665−570) cm^{-1} clearly arise from methyl rocking motions. Bands associated with $\nu_{as}(CH_3)$ and $\nu_s(CH_3)$ occur at relatively low frequencies (2932 and 2862 cm^{-1}, respectively), as do their CD_3 counterparts: corresponding features in the spectrum of CH_3ReO_3 occur at 2989 and 2899 cm^{-1}.[9a] The intensities of these features in IR absorption, their appearance in both CH_3 and CD_3 isotopomers, and the consistent agreement between experimental and calculated frequencies lead us to the confident conclusion that they represent fundamental modes, with no significant perturbation from Fermi

(5) Brown, S. D.; Green, P. J.; Gard, G. L. *J. Fluorine Chem.* **1975**, *5*, 203-219.

(6) Ward, T. R.; Bürgi, H.-B.; Gilardoni, F.; Weber, J. *J. Am. Chem. Soc.* **1997**, *119*, 11974−11985.

(7) (a) Herrmann, W. A.; Kühn, F. E.; Roesky, P. W. *J. Organomet. Chem.* **1995**, *485*, 243−251. (b) Rau, M. S.; Kretz, C. M.; Geoffroy, G. L.; Rheingold, A. L.; Haggerty, B. S. *Organometallics* **1994**, *13*, 1624−1634.

(8) McGrady, G. S.; Downs, A. J.; Scherer, W.; Haaland, A. To be published.

Table 1. Experimental and Calculated (DFT-GIAO) ^{1}H, ^{13}C, and ^{17}O Chemical Shifts δ (in ppm Relative to TMS) for $MeReO_3$, $EtReO_3$, and Me_3ReO_2

param (ppm)	$MeReO_3$ exp	BPW91/II calc	EtReO3 exp	BPW91/II calc	Me_3ReO_2 exp	BPW91/II calc
$\delta(CH_3)$	1.34[a]	1.75	1.29[b]	1.28	2.47/2.03[d]	1.76/0.94[e]
$\delta(CH_2)$			2.31[b]	2.45		
δC_α	19.0[d]	19.2	36.6[b]	39.8	29.7/26.7[d]	34.0/27.0[e]
δC_β			18.2[b]	21.1		
δO	829[d]	839	844[b,c]	843	756[d]	754
σRe		−213.4		−220.7		−210.1

[a] $C_6D_5CD_3$ solution. [b] C_6D_6 solution. [c] CD_2Cl_2 solution. [d] $CDCl_3$ solution. [e] Individual δ^1H values: 1.06 (H11), 0.86 (H12), 2.47 (H21), 1.44 (H22), and 1.37 (H23).

Table 2. Major Features in the Vibrational Spectrum of Me_3ReO_2[a]

$(CH_3)_3ReO_2$			$(CD_3)_3ReO_2$			
Ar matrix (IR)	liquid (Raman)	calc	Ar matrix (IR)	liquid (Raman)	calc	approximate description
3022 w	3025 m	3152				
3000 w		3152	2274 w			
	2991 ms	3132				$\nu_{as}CH_3$ (CD_3)
2968 m		3100, 3104	2267 mw	2270 ms	2335, 2331	
2932 m		3096	2243 mw	2237 ms	2294, 2287	
			2229 mw			
2911 m,sh		2982				
2881 m	2889 vs					ν_sCH_3 (CD_3)
2862 m		2967	2114 w	2109 vs	2137	
1469 mw		1489	1080 w		1081	
1460 mw		1446	1037 w		1051	$\delta_{as}CH_3$ (CD_3)
1404 mw	1406 mw	1435, 1440	1029 mw	1027 w	1045, 1042	
1396 m	1389 mw	1416, 1427	1021 w		1038, 1030	
1253 vw		1276	945 w			
1242 vw	1239 vw	1230	927 w	917 m	937, 935	δ_sCH_3 (CD_3)
1194 m	1193 mw	1225	906 vw			
1004 s	994 vs	976	1006 s	998 vs	979	ν_sReO_2
966 vs	956 mw	961	962 vs	942 m	954	$\nu_{as}ReO_2$
823 vw	825 m	839, 902	665 w		667	
			663 w			ρCH_3 (CD_3)
756 m		785, 797	640 w	641 m	658	
752 m	757 w	774	571 m	576 mw	598, 596, 590	
524 w,br	532 s	518, 522	478 mw	489 s	479	$\nu_{as}Re(C_{ax})_2$, $\nu_s[Re(C_{ax})_2 + ReC_{eq}]$[b]
484 vw	483 m	475		438 m	431	$\nu_s[Re(C_{ax})_2 - ReC_{eq}]$[b]
c	402 w	407	*c*	359 w	358	
c		290	*c*			
c	290 m	278	*c*	286 m	273	
c	269 ms	276	*c*			δC_3ReO_2
c	256 ms	255	*c*		239	
c	233 m,sh	229, 247	*c*	242 s	238	
c	215 mw	205	*c*	214 w	204	

[a] Energies in cm^{-1}; as = antisymmetric, s = symmetric, ν = stretching, δ = deformation, ρ = rocking, τ = torsion, v = very, s = strong, m = medium, w = weak, sh = shoulder. [b] See ref 10b. [c] No measurements made at energies below 400 cm^{-1}.

resonance, a complication that has beset the assignment of ν(CH) modes in the past.[9b] There are grounds therefore for believing that some C−H bonds are weakened by secondary interactions either with the oxo ligands or with the Re center (q.v.). The observed frequencies are remarkably close to those reported for (η^5-C_5H_5)$TiMe_3$, whose IR spectrum was interpreted in terms of a modest α-C−H···Ti agostic interaction,[9c] and comparable with those observed for $MeTiCl_3$(dmpe) (dmpe = $Me_2PCH_2CH_2PMe_2$), the structure of which clearly denotes an α-agostic interaction.[9d] On the other hand, they lie significantly higher than those reported for the β-agostic C−H bonds in the ethyl ligands of (η^5-$C_5Me_5)_2ScEt$[9e] and $EtTiCl_3$(dmpe).[9f] We note, however, that the study of (η^5-C_5H_5)$TiMe_3$ involved all four methyl group isotopomers CH_nD_{3-n} (n = 0−3) and studies in several phases;[9c] accordingly we prefer to await the results of a similar study on Me_3ReO_2 before drawing definitive conclusions on this point.

There are no anomalous features apparent in the methyl deformation modes observed for either the CH_3 or CD_3 isotopomer, but we note that the rocking vibrations appear at significantly higher wavenumber than do the corresponding modes of methyltitanium compounds,[11] probably reflecting greater directionality in the more covalent Re−C bonds.

(ii) Skeletal Vibrations. Assignment of two features in the IR spectrum to Re═O stretching vibrations

(9) (a) Herrmann, W. A.; Kiprof, P.; Rypdal, K.; Tremmel, J.; Blom, R.; Alberto, R.; Behm, J.; Albach, R. W.; Bock, H.; Solouki, B.; Mink, J.; Lichtenberger, D.; Gruhn, N. E. *J. Am. Chem. Soc.* **1991**, *113*, 6527−6537. (b) McKean, D. C. *Chem. Soc. Rev.* **1978**, *7*, 399−422; *Croat. Chem. Acta*, **1988**, *61*, 447−461. (c) McGrady, G. S.; Downs, A. J.; Hamblin, J. M.; McKean, D. C. *Organometallics* **1995**, *14*, 3783−3790. (d) McGrady, G. S.; Downs, A. J.; Scherer, W. Unpublished results. (e) Thompson, M. E.; Baxter, S. M.; Bulls, A. R.; Burger, B. J.; Nolan, M. C.; Santarsiero, B. D.; Schaefer, W. P.; Bercaw, J. E. *J. Am. Chem. Soc.* **1990**, *112*, 1289−1291. (f) McGrady, G. S.; Downs, A. J.; Haaland, A.; Scherer, W.; McKean, D. C. *J. Chem. Soc., Chem. Commun.* **1997**, 1547−1548.

(10) (a) Beattie, I. R.; Crocombe, R. A.; Ogden, J. S. *J. Chem. Soc., Dalton Trans.* **1977**, 1481−1489. (b) Casteel, W. J., Jr.; Dixon, D. A.; LeBlond, N.; Lock, P. E.; Mercier, H. P. A.; Schrobilgen, G. J. *Inorg. Chem.* **1996**, *35*, 4310−4322.

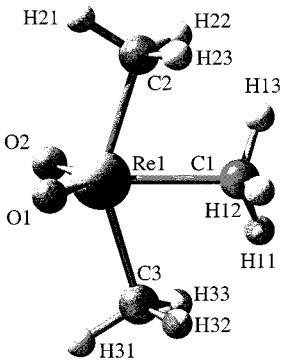

Figure 2. Molecular model of Me_3ReO_2, **1**, with C_s symmetry.

precludes a D_{3h} structure for the molecule with both oxo ligands in axial positions, **1a**. These vibrations occur at 1004 and 966 (1006 and 962) cm^{-1} in the matrix spectrum and are assigned as ν_s and ν_{as}, respectively, for the ReO_2 unit. The frequencies are very close to those reported for the corresponding modes in the molecules $[MO_2F_3]^{n+}$ [M = Re, $n = 0$; M = Os, $n = 1$),[10] $MeReO_3$,[9] and $(\eta^5\text{-}C_5Me_5)ReO_3$.[9] Clearly they offer no support for perturbations of type (ii). The relative intensities of the two absorptions, 2.90:1, lead us to an estimate of ca. 117° for the ∠OReO bond angle,[12] a value in fair agreement with the GED and DFT conclusions (q.v.), and with an earlier vibrational study of ReO_2F_3.[10] Prominent features at 532 and 489 (489 and 438) cm^{-1} in the Raman spectrum are assigned to Re−C stretching vibrations, the latter being ascribed to ν Re−C_{eq} and the former representing both the symmetric and antisymmetric Re−C_{ax} modes, which are calculated to be separated by no more than a few cm^{-1}. Several skeletal deformation and methyl torsion modes occur at wavenumbers below 450 cm^{-1}. Once again, though, none of these provides support for the existence of appreciable α-C−H···O═Re interaction in any form.

2.3. Molecular Structure of Me_3ReO_2 As Determined by DFT Calculations and GED Measurements. Structure optimizations by DFT calculations on an EBT model (**1e**) of C_s symmetry yielded the structure depicted in Figure 2 and the structure parameters listed in Table 3. Calculation of the molecular force field confirmed that this model corresponds to a minimum on the potential energy surface. We were unable to find any minimum on the potential energy surface (PES) corresponding to a SQP structure (**1d**). Optimizations on such models tended to converge to TBP models of C_{3h} symmetry (**1a**) with both O atoms in axial positions and a horizontal mirror plane formed by the ReC_3 fragment and one H atom of each methyl group. The energy of this C_{3h} structure although a minimum on the PES was, however, found to be 10.7 kcal mol^{-1} above the EBT minimum. An alternative C_{3v} model with three C−H bonds of each methyl group eclipsing the same Re═O bond was slightly less stable than the C_{3h} model (0.36 kcal mol^{-1} higher energy) and could be characterized as a saddle point on the PES (two imaginary frequencies). As we have seen, a TBP equilibrium structure like **1a** is ruled out by NMR spectra. In the EBT equilibrium structure the orientation of the equatorial methyl group appears to be such that one C−H bond is lying in the ReO_2 plane. The methyl group is tilted some 5° toward the O1 atom (the in-plane ∠ReCH12 valence angle is 103.4°, the out-of-plane angle ∠ReCH11 = 113.1°), and the valence angle ∠C_{eq}ReO1 = 116.6° is slightly smaller than ∠C_{eq}ReO2 = 119.3°, indicating, perhaps, a weak H12···O1 attraction. Moreover, the in-plane C−H12 bond appears to be slightly elongated relative to the out-of-plane C−H11 bond (1.107 vs 1.099 Å). The Re−O1 bond seems also to be slightly stretched (by 0.001 Å) in comparison with the Re−O2 bond, which is not involved in any H···O2 interaction.

The molecular fragment $ReO_2(C_{ax}H_3)_2$ appears to have near-perfect C_{2v} symmetry. The potential restricting internal rotation of the equatorial methyl group must therefore have 6-fold symmetry. The barrier height is then expected to be much smaller than the thermal energy available at the temperature of the GED experiment (RT = 0.6 kcal mol^{-1}); under these conditions the equatorial methyl group is expected to rotate freely, and the effective molecular symmetry should be C_{2v}. Structure refinements on the GED data were therefore based on an EBT model in which the equatorial methyl group was fixed in the orientation shown in Figure 2, but the rest of the molecule restrained to C_{2v} symmetry. The

Table 3. Interatomic Distances, Valence Angles, and rms Vibrational Amplitudes (*l*) in Me_3ReO_2, 1, Determined by Gas Electron Diffraction (GED) and DFT Calculations[a]

	r_a(GED)	r_e(DFT)[b]	*l*(GED)	*l*(DFT)
		Bond Distances		
Re−C_{eq}	2.199(22)	2.193	0.050(12)[d]	0.06
Re−C_{ax}	2.122(6)	2.130	0.048(12)[d]	0.058
Re═O	1.703(3)	1.739[c]	0.029(5)	0.036
C−H	1.115(9)	1.102[c]	0.066(11)	0.078
		Nonbonded Distances		
O···O	2.993(29)	3.071	0.037(33)	0.076
O···C_{ax}	2.896(12)	2.916[c]	0.11(2)[e]	0.115
O···C_{eq}	3.362(23)	3.377[c]	0.12(2)[e]	0.122
C_{ax}···C_{eq}	2.584(29)	2.610	0.12(5)[f]	0.091
C_{ax}···C_{ax}	4.068(28)	4.100	0.11(5)[f]	0.084
		Valence Angles		
∠C_{eq}ReC_{ax}	73.5(11)	74.3		
∠C_{eq}ReO	118.5(10)	118.0[c]		
∠C_{ax}ReC_{ax}	146.9(22)	148.5		
∠OReO	123.0(20)	124.0		
∠ReCH	106.5(13)	108.9[c]		
R-factors[g]	0.055 (50 cm)	0.143 (25 cm)	0.104 (total)	

[a] Distances and vibrational amplitudes in Å, angles in deg. Estimated standard deviations of GED parameters in parentheses in units of the last digit. As refinements were carried out with diagonal weight matrixes, the esd's have been tripled to reflect the added uncertainty due to data correlation and further expanded to include an estimated scale uncertainty of 0.1%. [b] BPW91/I calculation. [c] Average values. Individual distances (in Å) were Re−O1 = 1.739, Re−O2 = 1.738, C_{eq}−H11 = 1.099, C_{eq}−H12 = 1.107, C_{ax}−H21 = 1.109, C_{ax}−H22 = 1.099, C_{ax}−H23 = 1.098, C_{ax}−O1 = 2.910, C_{ax}−O2 = 2.922, C_{eq}−O1 = 3.354, and C_{eq}−O2 = 3.400. Individual angles (in deg) were ∠C_{eq}ReO1 = 116.6, ∠C_{eq}ReO2 = 119.3, ∠ReC_{eq}H11 = 113.1, ∠ReC_{eq}H12 = 103.4, ∠ReC_{ax}H21 = 100.8, ∠ReC_{ax}H22 = 111.1, and ∠ReC_{ax}H23 = 113.3. [d−f] The two amplitudes were refined with constant difference. [g] $R = (\sum w(I_{obs} - I_{calc})^2/\sum w I_{obs}^2)^{1/2}$.

(11) (a) McKean, D. C.; McQuillan, G. P.; Torto, I.; Bednall, N. C.; Downs, A. J.; Dickinson, J. M. *J. Mol. Struct.* **1991**, *247*, 73−87. (b) McGrady, G. S.; Downs, A. J.; Bednall, N. C.; McKean, D. C.; Thiel, W.; Jonas, V.; Frenking, G.; Scherer, W. *J. Phys. Chem. A* **1997**, *101*, 1951−1968.

(12) See, for example: Nakamoto, K. *Infrared and Raman Spectra of Inorganic and Coordination Compounds*, 5th ed.; Wiley: New York, 1997.

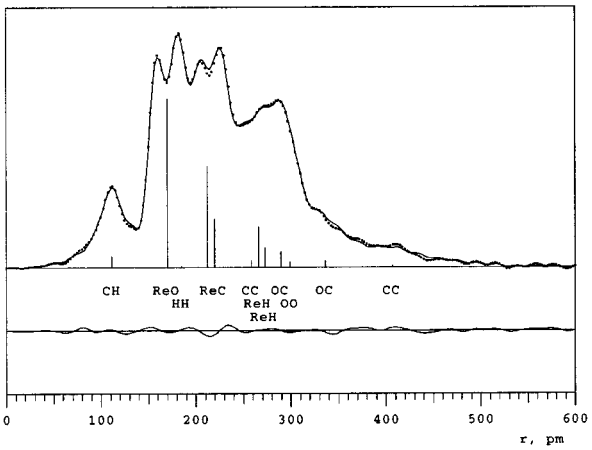

Figure 3. (top) Experimental (dots) and calculated (line) modified radial distribution curves for Me_3ReO_2 (**1**). The vertical scale is arbitrary. (bottom) Difference curve. Artificial damping constant $k = 0.0025$ Å^2. The structural refinements are based on a molecular model with C_s symmetry (Figure 2).

GED data do not permit the determination of individual C−H bond distances or ∠ReCH valence angles; only an average methyl group geometry could be refined. The final refinements yielded the structure parameters listed in Table 3. Experimental and calculated radial distribution curves are compared in Figure 3.

Several unsuccessful attempts were made to fit a SQP model with the O atoms at opposite corners of the base (**1d**) to the electron diffraction data. Full-matrix least-squares refinement of seven structure parameters and seven vibrational amplitudes as for the EBT model proved impossible without divergence. Stepwise refinements of a smaller set of parameters at a time led to *R*-factors greater than 0.16 as compared to 0.10 for the best EBT model and unreasonable values for several amplitudes, including bond distance amplitudes. We conclude that the SQP model is incompatible with the GED data.

The optimum geometry to which we are thus led reveals a large distortion of the idealized TBP coordination geometry: equatorial and axial methyl groups span $\angle C_{eq}ReC_{ax}$ angles of only 73.5(11)° at the metal center. The angle $\angle C_{ax}ReC_{ax}$ is 146.9(22)°, a value similiar to those found in **2** and **3** in the solid state [$\angle C_{ax}ReC_{ax}$ = 149.7(5)° and 145.4(2)°, respectively].[4a,b] The axial Re−C bonds emerge as being slightly but significantly shorter than the equatorial one [2.122(6) vs 2.199(22) Å by GED; 2.130 vs 2.193 Å by DFT calculations]. The equatorial bond distance is close to the Re−C bond distance in $(CH_3)_4ReO$, 2.117(3) Å,[13] but somewhat longer than the Re−C bond distance in CH_3ReO_3, 2.060(9) Å.[9]

Within the equatorial plane the ∠OReO angle is found to be 123.0(20)° [124.0° by DFT calculations] as compared to 117.4(5)° and 117.7(3)° in the solid-state structures of **2** and **3**, respectively.[4a,b] The difference hovers at the edge of statistical significance. If real, it may reflect the smaller steric demand of the organo groups in **1**. The Re═O bond distance at 1.703(3) Å is normal for dioxorhenium compounds.[14]

(13) Haaland, A.; Verne, H. P.; Volden, H. V.; Herrmann, W. A.; Kiprof, P. *J. Mol. Struct.* **1995**, *352/353*, 153−156.
(14) Mayer, J. M. *Inorg. Chem.* **1988**, *27*, 3899−3903.

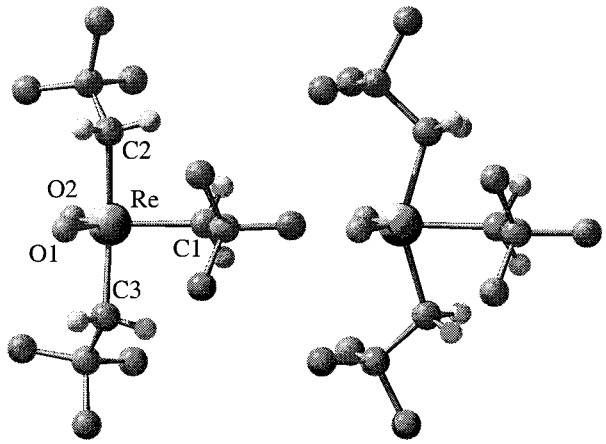

Figure 4. Comparison of the core geometries of $(Me_3CCH_2)_3ReO_2$, **2** (γ-H atom positions omitted for clarity). (left) Geometry determined by X-ray diffraction.[4a] Salient distances (Å) and angles (deg): Re═O1 = 1.812(11), Re═O2 = 1.661(9), Re−C2 = 2.137(12), Re−C1 = 2.175(14), Re−C3 = 2.118(14), ∠O1ReO2 = 117.4(5), ∠O1ReC1 = 108.8(5), ∠O2ReC1 = 133.8(6), ∠C2ReC1 = 86.5(2), and ∠C3ReC1 = 89.4(5). (right) Geometry calculated by the DFT (BPW91/I) method. Re═O1 = 1.676, Re═O2 = 1.686, Re−C2 = 2.126, Re−C1 = 2.192, Re−C3 = 2.126, ∠O1ReO2 = 120.2, ∠O1ReC1 = 130.3, ∠O2ReC2 = 109.5, ∠C2ReC1 = 76.1, and ∠C3ReC1 = 76.1.

The DFT calculations indicate that the axial methyl groups are nearly staggered with respect to the $C_{eq}ReO_2$ fragment [τ(H21−C_{ax}−Re−C_{eq} = −172.8°] and tilted in such a manner that the hydrogen atoms located in the vertical ReC_3 plane (H21 and H31) display remarkably small ∠ReCH angles of 100.8°. The in-plane C−H bond distances are enlarged by 0.010 Å relative to the four out-of-plane C−H bonds [1.109 vs 1.098−1.099 Å]. We return to a discussion of the origin of this tilt in the following section. There are no experimental signs of interaction between the axial methyl groups and the oxo ligands.

The structure of the solid neopentyl compound **2** (Figure 4) appears to be strikingly different: the axial neopentyl groups are oriented in such a fashion that one C_α−H bond in each substituent eclipses one of the Re═O bonds, and this bond distance is increased to 1.812(11) Å, making it apparently the longest Re═O bond recorded to date.[14] The other Re═O bond measuring 1.661(9) Å is normal. Both the orientation of the axial ligands and the elongation of the eclipsed Re═O bond were first interpreted as evidence for intramolecular α-C−H···O═Re attraction.[4a] We note, however, that Wierda and co-workers[4a] report two strong IR bands at 994 and 944 cm^{-1}, i.e., very close to the symmetric and antisymmetric Re═O stretching frequencies in **1** (see Table 2). Such an assignment would be incompatible, however, with the reported bond distances. More recently the crystal structure of the mixed neopentyl/phenyl derivative **3** has been determined.[4b] Here the phenyl group occupies an equatorial position, while the axial neopentyl groups are oriented in such a way that the bonds radiating from the α-carbon atoms are approximately staggered with respect to the ReO_2C_{eq} fragment and the C_α−C_β bonds are *anti* with respect to the Re−C(phenyl) bond. The two Re═O bond distances are normal, and the IR spectrum displays two bands at 987 and 945 cm^{-1}. Wierda and co-workers have there-

Table 4. Highest Occupied Molecular Orbitals in $(CH_3)_3ReO_2$, 1

orbital	symmetry	description (major/minor contributions)
HOMO	3a′	σ Re−C_{eq}/O p (in plane)[a,b]
HOMO-1	2a″	σ Re−C_{ax}/π* Re−O (out of plane)[b]
HOMO-2	2a′	O p (in plane)[b]
HOMO-3	1a″	π Re−O (out of plane)[b]/C−H···Re
HOMO-4	1a′	σ Re−C_{ax}

[a] O p denotes 2p atomic orbitals on O atoms. [b] (in plane) or (out of plane) denotes p- or π-orbitals with the maximum electron density in or out of the equatorial symmetry plane, respectively.

fore suggested that the conformation of **2** is determined by steric interaction between the organic ligands and that the exceptionally long Re═O bond is due to a crystallographic error.[4b]

We have optimized the structure of **2** by DFT calculations starting with the structure obtained by X-ray diffraction. The orientation of the equatorial neopentyl group did not change during optimization, but the two axial neopentyl groups rotated into the staggered orientation displayed by **3** (see Figure 4). The two Re═O distances converged to 1.676 and 1.686 Å. Accordingly, we conclude that the crystal structure of **2** should be redetermined before it can be regarded as established.

2.4. Metal-to-Ligand Bonding. Ward and co-workers have surveyed the crystal structures of 36 compounds each containing a pentacoordinated early transition metal (groups 4 through 7) with a d^0 configuration with two strongly π-bonding and three σ-bonding or weakly π-bonding ligands.[6] In five compounds the two strongly π-bonding ligands are found to occupy axial positions; in the remaining 31 they occupy equatorial positions, while the coordination geometries map out the transition from TBP (as in **1c**) to EBT (as in **1e**) configurations.[6] We note that their sample contains 21 compounds where both the strongly π-bonding ligands are double-faced and that all of these, like Me_3ReO_2, fall into the EBT category. Ward and co-workers carried out extended Hückel and DFT calculations on the model complex $[H_3Ti(NH_2)_2]^-$ with the lone pairs on the planar-NH_2 units pointing out of the equatorial symmetry plane and traced the deformation from TBP to EBT coordination geometry to the interaction between the π-orbitals on the N atoms, the d_{yz} orbital of the metal atom, and the fragment molecular orbitals (FMO) of the axial H atoms.[6]

Since Me_3ReO_2 is the simplest EBT d^0 transition element compound to be characterized structurally up to the present time, we decided to investigate whether the conclusions reached by Ward and co-workers are valid for a real system. In addition to searching for an explanation for the distortion from an ideal TBP to EBT coordination geometry, we were also looking for the origin of the tilt assumed by the axial methyl groups.

The symmetry and nature of the five highest occupied molecular orbitals are described in Table 4 and displayed in Figure 5 which also indicates how the orbitals may be formed from the molecular orbitals of the O_2ReC_{eq} and $(C_{ax})_2$ fragments. In the following discussion we shall be particularly interested in the two orbitals that provide bonding between the metal atom and the axial C atoms, viz., the 2a″ HOMO-1 and 1a′ HOMO-4 orbitals. The former may be described as a

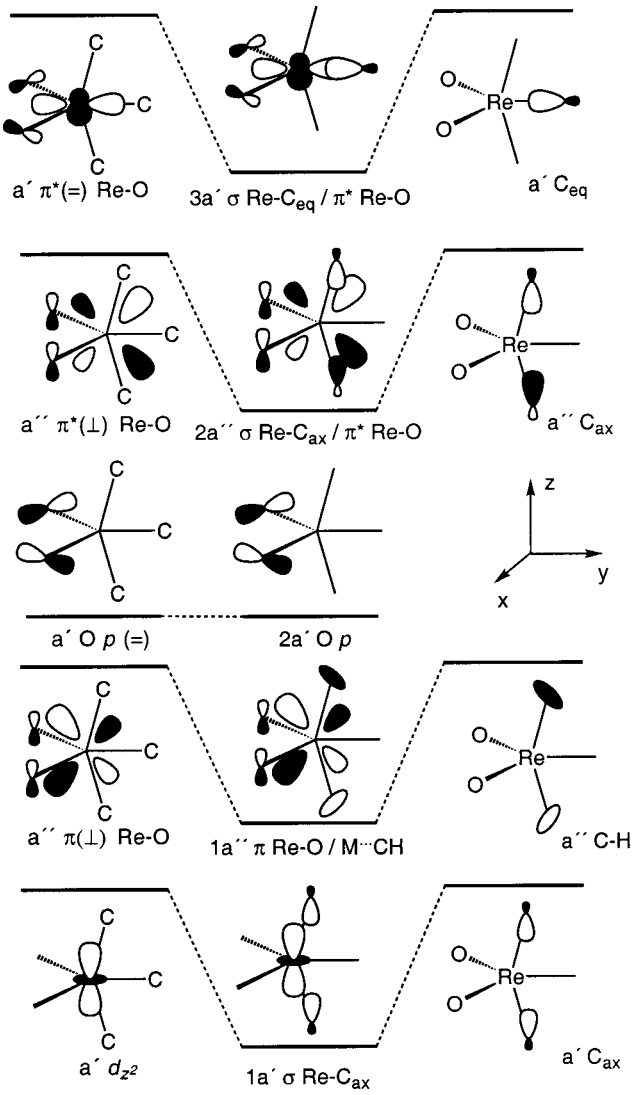

Figure 5. Construction of the five highest occupied molecular orbitals (HOMOs) of Me_3ReO_2, **1**. Oxygen atom p-orbitals and Re−O π-orbitals with maximum electron density out of the ReO_2 plane are denoted by "⊥", those with maximum electron density in the plane by "═".

combination of the a″ C_{ax} FMO and the a″ π* Re−O orbital; this π* orbital is composed in turn of the Re d_{yz} orbital, which is polarized away from the O atoms in antibonding combination with a smaller amount of the out-of-plane p orbitals on the O atoms. The HOMO-4 may be described as the simple combination of the a′ C_{ax} FMO and the d_{z^2} atomic orbital on Re.

Structure optimization of a TBP model, i.e., a model where the $C_{ax}ReC_{ax}$ fragment is constrained to linearity, yields an energy 24.7 kcal mol^{-1} above that of the equilibrium structure. The energy of the 2a″ Re−C_{ax} σ-bonding orbital increases by 1.09 eV, and the Re−C_{ax} bond distances increase by about 0.08 Å to 2.212 Å. At the same time the energy of the 3a′ Re−C_{eq} σ-bonding orbital decreases by 0.35 eV and the Re−C_{eq} bond distance decreases by about 0.07 Å to 2.120 Å. The energies of the other orbitals in Table 4 change by less than 0.25 eV. We conclude that the driving force for distortion from TBP to EBT coordination is provided by the electrons in the 2a″ Re−C_{ax} σ-bonding orbital and suggest that the stabilization of the EBT geometry is due to improved overlap between the a″ C_{ax} FMO and

the d_{yz} orbital on the Re atom. The overlap is at its maximum if the valence angle $\angle C_{eq}ReC_{ax}$ is 45°. Reduction of this angle to optimize the overlap results, however, in a decrease of the overlap between the a′ FMO of the axial C atoms and the Re d_{z^2} orbital, which is at its maximum when $\angle C_{eq}ReC_{ax}$ is 90°. Overall, we believe the observed angle of 73.5(11)° represents a compromise between optimal bonding by means of the d_{z^2} and d_{yz} AO's on Re. We also suggest that distortion along the negative pseudorotation coordinate to the EBT geometry is favored over distortion along the positive pseudorotation coordinate to the SQP geometry for two reasons: (i) it allows overlap between the a″ C_{ax} FMO and the major lobes of the polarized d_{yz} orbital, and (ii) distortion along the positive pseudorotation coordinate would lead to antibonding $C_{ax}\cdots O_{eq}$ interactions (see Figure 5).[15]

We now turn our attention to the tilting of the axial methyl groups. Distortions of this type, which have been found increasingly often in transition metal methyl complexes, are commonly interpreted in terms of an attractive, so-called α-agostic, C−H···M interaction.[16] Indeed, the term "α-agostic" is sometimes used to describe any tilted methyl group that is bonded to a transition metal. We believe, however, that it would be wise to distinguish between the description of the geometry (i.e., tilted methyl group) and the cause of the tilting, which may not always be due to C−H···M attraction.

The optimal TBP model with a linear $C_{ax}ReC_{ax}$ fragment displays greater methyl tilting than does the equilibrium structure, with ∠ReCH21 = 94.0° versus 100.8°. Optimization of a model where $\angle C_{ax}ReC_{ax}$ is constrained to linearity and methyl tilting prevented by fixing ∠ReCH21 at 109.5° leads to an energy increase of 4.7 kcal mol^{-1}. At the same time the energy of the 2a″ Re−C_{ax} σ-bonding orbital increases by 0.10 eV, while the energies of the other orbitals in Table 4 decrease. We suggest therefore that the driving force for tilting of the axial methyl groups—like the distortion from TBP to EBT coordination geometry—is provided by the electrons in the 2a″ Re−C_{ax} σ-bonding orbital. In Figure 6 (left) we display the constant density contours of the 2a″ orbital of the TBP model with a linear $C_{ax}ReC_{ax}$ fragment in the ReC_3 plane. It is clear that the tilting has increased the overlap between the a″ C_{ax} FMO and the d_{yz} orbital on Re. The resulting density contours indicate that the Re−C_{ax} bonds are bent; the maximum electron density path between the atoms does not fall on a straight line between the nuclei. The tilting of the axial methyl groups in the configuration with $\angle C_{ax}ReC_{ax} = 180°$ may therefore be regarded as a consequence of the bent Re−C_{ax} bonds (due in turn to the directional characteristics of the Re d_{yz} orbital). Inspection of the electron density contours of the 2a″ σ Re−C_{ax} bonding orbital of the optimal EBT configuration appears to confirm this point.

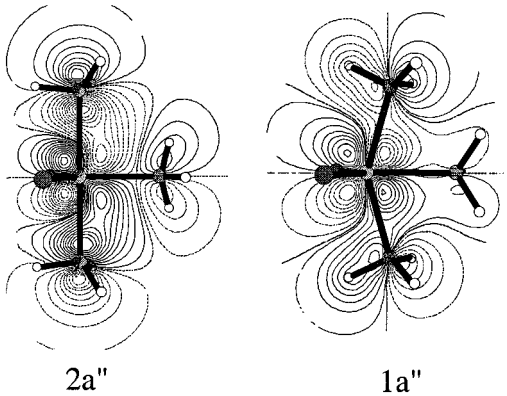

Figure 6. Constant probability density contour map of molecular orbitals in the ReC_3 plane. (left) 2a″ σ Re−C_{ax} MO of an optimized TBP model ($\angle C_{ax}ReC_{ax} = 180°$). (right) 1a″ MO of the optimized EBT (equilibrium) structure ($\angle C_{ax}ReC_{ax} = 148.5°$).

Optimization of an EBT model in which ∠ReCH21 is fixed at 109.5° yielded an energy 1.8 kcal mol^{-1} above the equilibrium geometry. At the same time the energy of the 1a″ molecular orbital increases marginally (by 0.002 eV), while the energies of the other orbitals in Table 4 decrease; it appears that the stabilization due to tilting of the axial methyl groups is less than half that of the TBP model. In Figure 6 (right) we display constant density contours of the 1a″ π Re−O molecular orbital in the ReC_3 plane: an agostic C−H···Re bonding interaction is clearly indicated. Agostic interactions are often assumed to arise from the donation of "extra" electron density previously located on the alkyl substituent into a vacant orbital on the electron-deficient metal atom. Such an interaction is not expected in Me_3ReO_2, which displays the chemical properties of an electronically saturated metal center. In the present case, the C−H···Re bonding interaction, if real, is due to delocalization of metal−ligand bonding electrons; the number of electrons in the valence shell of the metal atom remains unaltered.[17] Accordingly we suggest that the tilting of the axial methyl groups in Me_3ReO_2 may be due in part to weak C−H···Re agostic (bonding) interactions as well as to bending of the Re−C_{ax} bonds.

3. Experimental Section

All experiments were carried out using standard Schlenk, inert atmosphere, or high-vacuum techniques. Hexamethyltrioxodirhenium(VI) and dimethylzinc were prepared according to literature methods.[18] Other chemicals were used as purchased from commercial sources. Solvents were dried by literature methods. Dirhenium heptoxide and trimethylamine-*N*-oxide were purified by sublimation immediately prior to use.

NMR spectra were recorded using a JEOL JNM GX-400 spectrometer. IR spectra were measured for samples isolated in solid Ar matrixes at 12 K at dilutions of ca. 1000:1 using a

(15) Our conclusions are similar to those reached by Ward and coworkers on the basis of extended Hückel calculations on the model complex $[H_3Ti(NH_2)_2]^-$.[6] We note, however, that the ordering and nature of the molecular orbitals in the two species differ on essential points. In the real complex the a″ Re−C_{ax} σ-orbital lies above the a″ Re−O π-bonding orbital, while in the model complex the Ti−N π-orbital is higher than the a″ σ-TiH_{ax} orbital. Second, the a″ Ti−H_{ax} orbital is nonbonding with respect to the N atoms, while the a″ C_{ax} orbital in **1** is antibonding with respect to the O atoms.

(16) (a) Brookhart, M.; Green, M. L. H. *J. Organomet. Chem.* **1983**, *250*, 395−408. (b) Brookhart, M.; Green, M. L. H.; Wong, L.-L. *Prog. Inorg. Chem.* **1988**, *36*, 1−124.

(17) Constant-probability-density contour maps of molecular orbitals likewise indicate that the β-agostic effect in $EtTiCl_3$(dmpe) is due to delocalization of the M−C bonding electrons. See: Haaland, A.; Scherer, W.; Ruud, K.; McGrady, G. S.; Downs, A. J.; Swang, O. *J. Am. Chem. Soc.* **1998**, *120*, 3762−3772.

(18) (a) Herrmann, W. A.; Kuchler, J. G.; Felixberger, J. K.; Herdtweck, E.; Wagner, W. *Angew. Chem., Int. Ed. Engl.* **1988**, *27*, 394−396. (b) Hota, N. K.; Willis, C. J. *J. Organomet. Chem.* **1967**, *9*, 169−170.

Nicolet Magna-IR 560 spectrometer at a resolution of 1 cm^{-1}. Raman spectra were recorded for neat liquid samples using a Dilor Labram instrument at a resolution of 4 cm^{-1}. Mass spectra were measured at 70 eV using a Finnigan MAT 311-A instrument. Elemental analyses were performed in the microanalytical laboratory of the Inorganic Chemistry Department of the Technical University of Munich.

Synthesis of Trimethyldioxorhenium(VII). Anhydrous trimethylamine-*N*-oxide (38 mg; 0.50 mmol) was added to a solution of hexamethyltrioxodirhenium(VI)[3] (130 mg; 0.25 mmol) in ether (10 cm^3) maintained at −78° C. The resulting red solution was stirred for 30 min and then warmed to room temperature. Over a period of 2 h the color of the solution lightened gradually from red to yellow. Production of a clear yellow solution indicated completion of the reaction. Removal of the solvent in vacuo at −40° C produced a red-yellow oil, which was washed with water to remove excess trimethylamine-*N*-oxide, then purified by trap-to-trap fractionation in vacuo. Yield: 125 mg [90% based on the quantity of hexamethyltrioxodirhenium(VI) taken]. Anal. Calcd for $C_3H_9O_2Re$: C 13.68, H 3.45, Re 70.72. Found: C 14.06, H 3.4, Re 68.68%.

Quantum-Chemical Calculations. Calculations were carried out using the program system Gaussian 94.[19] Geometries were optimized at the BPW91 level of density functional theory (DFT) with the gradient correction of Becke[20a−c] for exchange and of Perdew-Wang[20d] for correlation. A quasi-relativistic effective core potential (ECP) and basis set from Hay and Wadt[21] were used for Re in conjunction with Dunning bases[22] on C, O, and H. This is our standard basis set and will be denoted "I" in the following. Additional calculations employed the effective core potentials (ECP) from Stoll and Preuss[23] for Re and standard 6-31G(d)[24] bases for C, O, and H (basis set denoted "II"). All Gaussian basis sets employed are listed in the Supporting Information. The initial BPW91/I optimizations for **1** were carried out without symmetry restriction and started from geometries without any symmetry. Invariably, however, the optimization converged to C_s symmetry. Thus, the final molecular geometry was optimized at different levels of theory within the constraints of the C_s point group. **2** was optimized at the BPW91/I level of theory without symmetry restraints. The DFT Cartesian force constants and Cartesian dipole moments were determined at the theoretical equilibrium geometries of **1** using numerical differentiation methods. The DFT force field of **1** was used to calculate the rms vibrational amplitudes and force constants through the program ASYM20.[25] A single scale factor for the theoretical force field of **1** was introduced and optimized (0.93) by minimizing the root-mean-square deviations between the calculated and observed frequencies. ^{13}C and ^1H chemical shifts were calculated at the BPW91/II level of theory for the BPW91/II-optimized structures using the gauge-independent atomic orbital (GIAO) method in Gaussian 94. Chemical shifts are given with respect to $Si(CH_3)_4$ (C,H) and H_2O (O) at the same computational level. Absolute shieldings of C and H in $Si(CH_3)_4$ at this level are 188.5758 and 32.2461, respectively; the absolute shielding of O in H_2O at the same level is 303.682.

Gas-Phase Electron Diffraction. Electron-diffraction measurements on trimethyldioxorhenium(VII) vapor were carried out with the Balzers KDG-2 unit at Oslo,[26] with the sample reservoir at 296 K, the vapor being injected in the dark via an all-glass inlet system held at room temperature. Exposures were made at nozzle-to-plate distances of ca. 50 cm (4 plates) and 25 cm (3 plates). The plates were traced using a modified Joyce-Loebl microdensitometer and the data processed with a program written by T. G. Strand. Atomic scattering factors were taken from ref 27. Backgrounds were drawn as least-squares-adjusted polynomials to the difference between the total experimental and the calculated molecular scattering intensities. Least-squares refinements were carried out with the program KCED26 written by G. Gundersen, S. Samdal, H. M. Seip, and T. G. Strand.

Structure refinements on the Me_3ReO_2 molecule were based on a molecular model in which the C_3ReO_2 frame was restricted to C_{2v} symmetry (see Figure 2). The axial methyl groups were fixed in staggered orientations, while the equatorial methyl group was fixed with one C−H bond in the equatorial plane, as forecast by the BPW91/I DFT calculations; the equatorial H atoms reduce the overall molecular symmetry to C_s. The DFT calculations indicated that the 9 C−H distances differ by less than 0.01 Å. Accordingly, the GED model was assumed to have one common C−H bond distance and local C_{3v} symmetry for each of the three methyl groups. The molecular structure was then determined by seven independent parameters, namely, the bond distances $Re-C_{ax}$, $Re-C_{eq}$, Re═O, and C−H and the valence angles $\angle OReC_{eq}$, $\angle C_{eq}ReC_{ax}$, and ∠ReCH. All intramolecular distances and vibrational amplitudes were included in the refinements. Experimental and calculated radial distribution curves are depicted in Figure 3.

Acknowledgment. We are grateful to the Deutsche Forschungsgemeinschaft for a postdoctoral fellowship (to W.S.), to Jesus College, Oxford, for a Research Fellowship (to G.S.M.), the VISTA program of STATOIL, and the Norwegian Academy of Science and Letters for financial support. The Norwegian Research Council has given support through a generous grant of computing time.

Supporting Information Available: Optimized geometries of Me_3ReO_2 at different levels of theory; GED intensity curves for Me_3ReO_2; basis set information. This material is available free of charge via the Internet at http://pubs.acs.org.

OM9904201

(19) Frisch, M. J.; Trucks, G. W.; Schlegel, H. B.; Gill, P. M. W.; Johnson, B. G.; Robb, M. A.; Cheeseman, J. R.; Keith, T. A.; Petersson, G. A.; Montgomery, J. A.; Raghavachari, K.; Al-Laham, M. A.; Zakrzewski, V. G.; Ortiz, J. V.; Foresman, J. B.; Cioslowski, J.; Stefanov, B. B.; Nanayakkara, A.; Challacombe, M.; Peng, C. Y.; Ayala, P. Y.; Chen, W.; Wong, M. W.; Andres, J. L.; Replogle, E. S.; Gomperts, R.; Martin, R. L.; Fox, D. J.; Binkley, J. S.; Defrees, D. J.; Baker, J.; Stewart, J. P.; Head-Gordon, M.; Gonzales, C.; Pople, J. A. *Gaussian 94*, Revision C.2; Gaussian, Inc.: Pittsburgh, PA, 1995.

(20) (a) Becke, A. D. *Phys. Rev.* **1988**, *A38*, 3098−3100. (b) Becke, A. D. *ACS Symp. Ser.* **1989**, *394*, 165−179. (c) Becke, A. D. *Int. J. Quantum Chem.* **1989**, *Symp. No. 23*, 599−609. (d) Perdew, J. P.; Wang, Y. *Phys. Rev.* **1992**, *B45*, 13244−13249.

(21) (a) Hay, P. J.; Wadt, W. R. *J. Chem. Phys.* **1985**, *82*, 270−283. (b) Wadt, W. R.; Hay, P. J. *J. Chem. Phys.* **1985**, *82*, 284−298. (c) Hay, P. J.; Wadt, W. R. *J. Chem. Phys.* **1985**, *82*, 299−310.

(22) Dunning, T. H., Jr.; Hay, P. J. In *Modern Theoretical Chemistry*; Schaefer, H. F., III, Ed.; Plenum: New York, 1977; Vol. 3, p 1.

(23) (a) Dolg, M.; Wedig, U.; Stoll, H.; Preuss, H. *J. Chem. Phys.* **1987**, *86*, 2123-2131. (b) Andrae, D.; Häussermann, U.; Dolg, M.; Stoll, H.; Preuss, H. *Theor. Chim. Acta* **1990**, *77*, 123−141.

(24) (a) Ditchfield, R.; Hehre, W. J.; Pople, J. A. *J. Chem. Phys.* **1971**, *54*, 724−728. (b) Hehre, W. J.; Ditchfield, R.; Pople, J. A. *J. Chem. Phys.* **1972**, *56*, 2257−2261. (c) Hariharan, P. C.; Pople, J. A. *Theor. Chim. Acta* **1973**, *28*, 213−222.

(25) Hedberg, L.; Mills, I. M. *J. Mol. Spectrosc.* **1993**, *160*, 117−142.

(26) (a) Zeil, W.; Haase, J.; Wegmann, L. *Z. Instrumentenk.* **1966**, *74*, 84−88. (b) Bastiansen, O.; Graber, R.; Wegmann, L. *Balzers High Vac. Rep.* **1969**, *25*, 1−8.

(27) Ross, A. W.; Fink, M.; Hilderbrandt, R. In *International Tables for Crystallography*; Wilson, A. J. C., Ed.; Kluwer Academic Publishers: Dordrecht, 1992; Vol. C, p 245.